Supplementary Information

Lightweight Copper–Carbon Nanotube Core–Shell Fiber for Power Cable Application

Kavitha Mulackampilly Joseph [1], Kyle Brittingham [1], Vamsi Krishna Reddy Kondapalli [1], Mahnoosh Khosravifar [1], Ayush Arun Raut [1], Brett David Karsten [2], Hunter J Kasparian [3], Nhat Phan [3], Arun Kamath [4], Amjad S. Almansour [5], Maricela Lizcano [5], Diana Santiago [5], David Mast [6], Vesselin Shanov [1, 3,*]

1 Department of Mechanical and Materials Engineering, University of Cincinnati, Cincinnati, OH 45221, USA; josephka@mail.uc.edu (K.M.J.)
2 Department of Chemistry, University of Cincinnati, Cincinnati, OH 45221, USA
3 Department of Chemical and Envionmental Engineering, University of Cincinnati, Cincinnati, OH 45221, USA
4 Department of Chemical and Biomolecular Engineering, University of California Berkeley, Berkeley, CA 94720, USA
5 Glenn Research Center, NASA, Cleveland, OH 44135, USA
6 Department of Physics, University of Cincinnati, Cincinnati, OH 45221, USA
* Correspondence: shanovvn@ucmail.uc.edu

S1. Palladium Decoration by Electroless Deposition

S1.1. Schematic of Palladium decoration

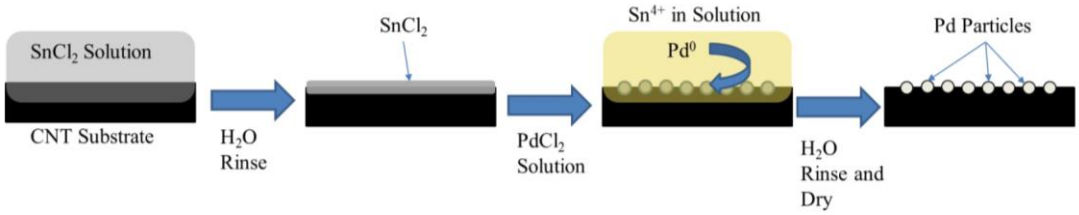

Figure S1. Schematic of palladium decoration on CNT by electroless deposition. Reproduced with permission from [1].

S1.2. Mechanism of palladium decoration

Electroless decoration of the functionalized CNT was done to obtain a dense copper coating on the CNT surface. The electroless deposition was accomplished by a two-step sensitization-activation method wherein the Sn sensitizing layer increased the palladium adsorption onto the CNT surface, simultaneously increasing the binding strength of the Pd–CNT interface. The Sn (2) species also reduced Pd (2) to Pd (0). The mechanism of the two-step sensitization-activation procedure reproduced from [2] is given in Fig. S2.

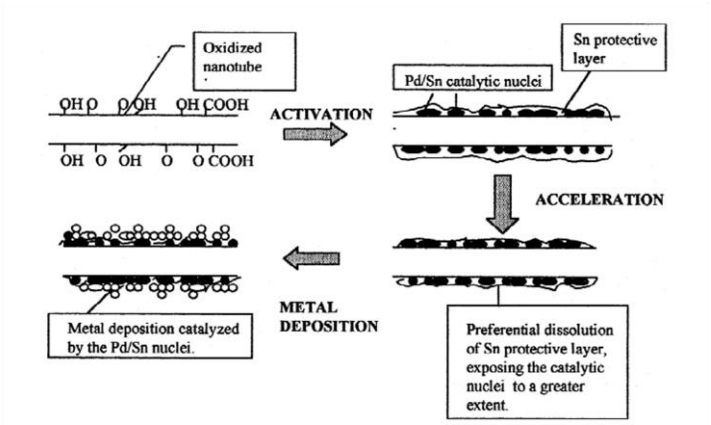

Figure S2. Mechanism of palladium decoration on CNT fiber by electroless deposition. Reproduced with permission from [2].

The palladium-seeded CNT fiber underwent an initial seeding of copper followed by a dense and homogenous continuous copper deposition to form the Cu–CNT composite fiber due to the high surface coverage of Pd–Sn nuclei on the activated CNT fiber.

S1.3. Energy Dispersive Spectroscopy(EDS) of Pd–Cu–CNT fiber

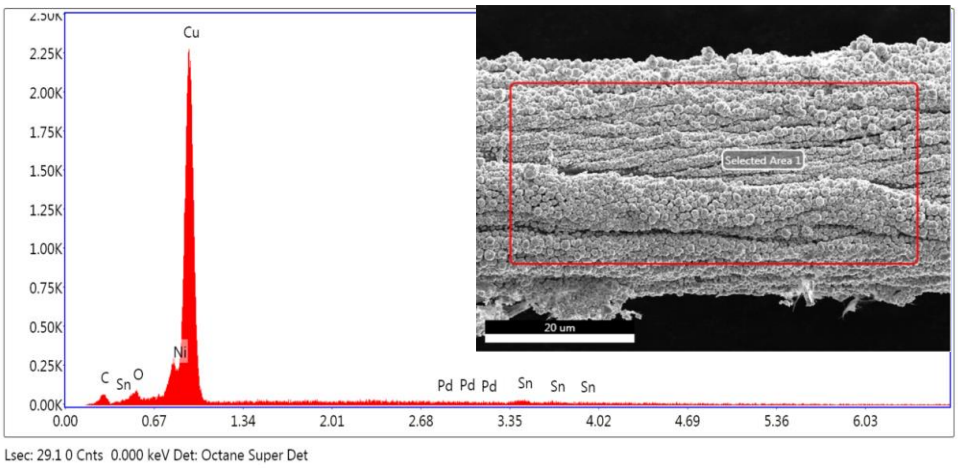

Figure S3. EDS of Pd–Cu–CNT fiber.

S2. Current density measurements

S2.1. Method

Initially, tests were performed in the ±2 mA range with increments of 0.1 mA every 2–3 seconds. Subsequent tests were performed with extended ranges of ±50 mA and ±100 mA, each with a step size of 1 mA. Experiments in large current ranges were repeated if a hysteresis was observed in the voltage–current plot. Further, a powerful power supply, HP 6114A, controlled via a varistor (10 mA increments every 5–10 seconds), along with an HP 34401A multimeter, was used to measure the maximum current density of the CNT fibers. The maximum current was recorded as the value just before the current reached the point of burnout. The maximum ampacity (maximum current density), ρ_I, was calculated by dividing the maximum current before burnout, I_{max}, by the cross-sectional area, A, as shown in the equation below. The cross-sectional area was assumed to be circular and was calculated from the fiber's diameter, D. The values for current density are reported in units of A/cm^2.

$$\rho_I = \frac{I_{max}}{A} = 4\frac{I_{max}}{\pi D^2}$$

S2.2. Current Density Test Setup with the Sample After Burnout

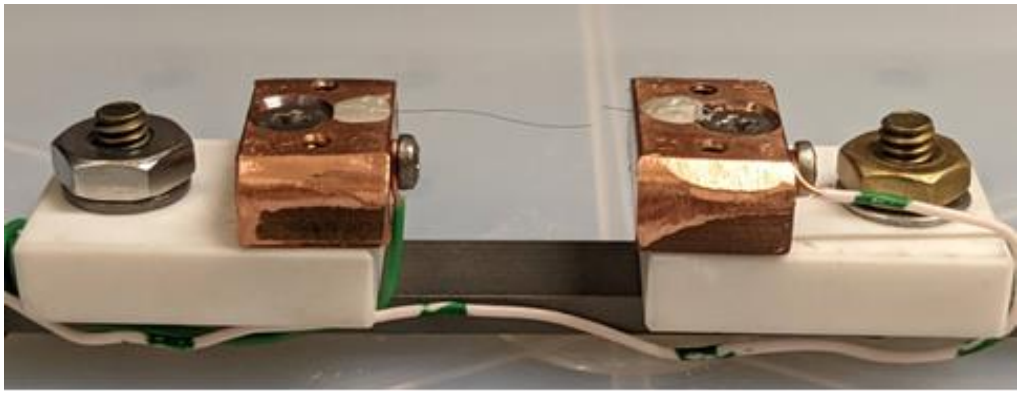

Figure S4. CNT sample after burnout on a current density measurement setup. Gap between copper mounting blocks is approximately 1.5 cm.

S2.3. Energy Dispersive Spectroscopy (EDS) of burnout Sample

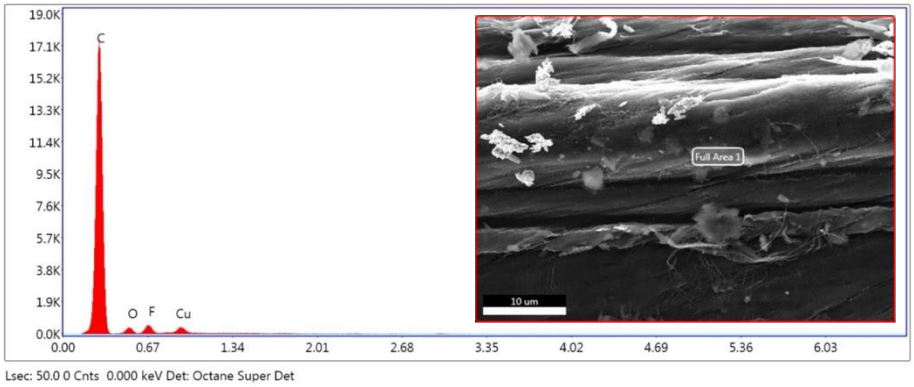

Figure S5. EDS of burnout sample after current density test.

S2.4. Current Density and Joule Heating

Current density measurements were performed on densified CNT fibers, unannealed Cu–CNT, and unannealed Pd–Cu–CNT fibers. Joule heating in the fibers resulted in an incandescent glow at currents greater than 40 mA. With the increase in current, the brightness of the glow intensified, and a color shift was observed from reddish orange to bright white. During the ±50 mA and ±100 mA tests, the densified CNT fiber exhibited a slight hysteresis in its voltage–current plot between 0 and +20 mA, shown in Fig. S6 a. The Cu–CNT and Pd–Cu–CNT samples exhibited a more pronounced hysteresis during the initial climb from 0 mA to +50 or +100 mA (Fig. S6 b). However, this was not observed when the current was decreased from 0 to −50 nor 0 to −100 mA during the same test. (Fig. S6 c.), which confirmed that the samples appeared to be conditioned by repetitive tests.

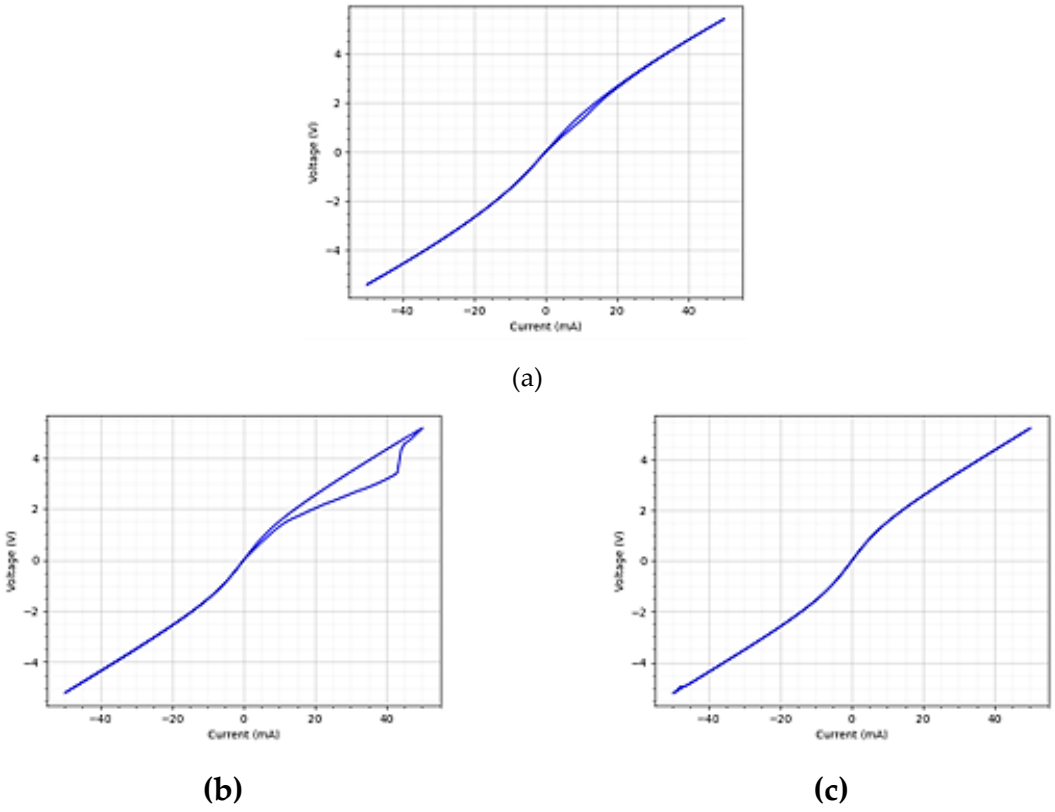

Figure S6. Examples of hysteresis seen in voltage–current plots. (a) Initial (±50 mA) test on a densified CNT sample with a marginal hysteresis between 0 and 20 mA. (b) Initial (±50 mA) test on a Cu–CNT sample, hysteresis observed on the first climb to 50 mA. (c) A repeat test (±50 mA) on the same Cu–CNT sample, where ahysteresis was not observed.

The intensity of the hysteresis in the plot was likely linked to the copper cladding, as it was marginal in the plots of the densified CNT fibers. The less substantial hysteresis observed in the densified CNT V–I plot could have been caused by the Joule heating resulting in an irreversible change, such as the desorption of moisture or relaxation of internal stresses. The higher intensity hysteresis seen in copper-coated samples could have been due to evaporation or sublimation of copper from the composite fiber due to intense Joule heating in the vacuum environment [3, 4]. The loss of copper from the composite's surface explains why the V–I plots of the copper-coated CNTs look very similar to that of the densified CNT fiber.

S3. Microtome Cutting

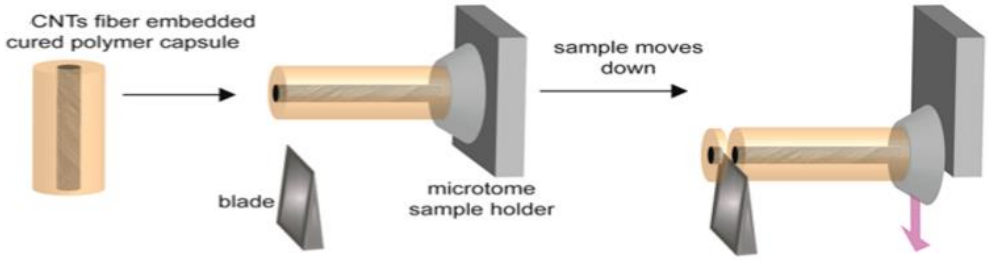

(a)

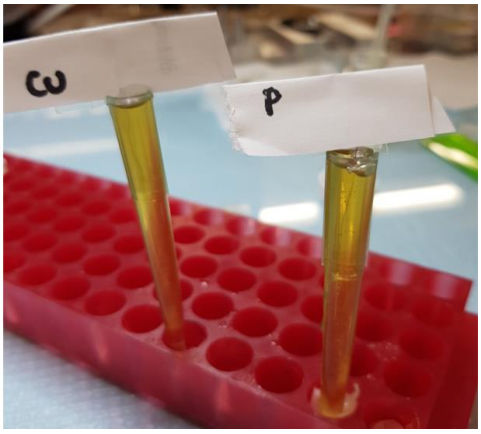

(b)

(c)

Figure S7 (a) Schematic of cutting by microtome (reproduced with permission from [5]). (b) Polymer-embedded Cu–CNT fiber and polymer-embedded CNT fiber. (c) Picture of the microtome.

References

1. McConnell C, Kanakaraj SN, Dugre J, Malik R, Zhang G, Haase MR, et al. *Hydrogen Sensors Based on Flexible Carbon Nanotube-Palladium Composite Sheets Integrated with Ripstop Fabric*. CS Omega 2020; 5:487–97. https://doi.org/10.1021/acsomega.9b03023
2. Ang LM, Hor TSA, Xu GQ, Tung CH, Zhao SP, Wang JLS. *Decoration of activated carbon nanotubes with copper and nickel* Carbon vol. 38. 2000; 363-372
3. Greenwood, H. C. and Rutherford, E. *The influence of Pressure on the Boiling Points of Metals.* Proceedings of the Royal Society of London. Series A, Containing Papers of a Mathematical and Physical Character 83, 565, pages 483-491 (1910) doi.org/10.1098/rspa.1910.0037
4. Kaye, George William Clarkson and Ewen, Donald and Glazebrook, Richard Tetley. *The sublimation of metals at low pressures.* Proceedings of the Royal Society of London. Series A, Containing Papers of a Mathematical and Physical Character 89, 607, pages 58-67 (1913) doi.org/10.1098/rspa.1913.0063
5. Gupta P, Rahm CE, Griesmer B, Alvarez, et al. *Carbon Nanotube Microelectrode Set: Detection of Biomolecules to Heavy Metals*. Anal Chem 2021; 93:7439–48 2021; 93:7439–48. https://doi.org/10.1021/acs.analchem.1c00360